Polish Society of Composite Materials
Polskie Towarzystwo Materiałów Kompozytowych

17: 2 (2017) 97-102

COMPOSITES THEORY AND PRACTICE

Tomasz Nowak

ABB - Corporate Research Center, ul. Starowiślna 13a, Krakow, Poland
Corresponding author. E-mail: tomasz.nowak@pl.abb.com

Received (Otrzymano) 12.12.2016

CLOSED-FORM SOLUTION FOR ELASTIC-PLASTIC ANALYSIS OF SELECTED FIBER METAL LAMINATES DURING LOADING-UNLOADING CYCLE

Fiber reinforced polymer composites and aluminum alloys nowadays constitute the most dominant materials applied in the aerospace industry. This paper gives the theoretical background and provides both analytical and numerical calculations for analysis of the elastic-plastic behavior of a selected fiber metal laminate. The work introduces the closed-form solution for a multi-layered structure subjected to a unidirectional loading/unloading cycle, and explains the process of stress and strains development. GLARE® plates, which are exposed to a tensile load, can generate even higher stress in the aluminum layers at unloading. Moreover, delamination and buckling of the external layers can be expected. The paper gives a detailed theoretical framework for this behavior based on the plasticity theory, provides numerical calculations, and compares them with the FEM and experimental results.

Keywords: **elastic-plastic behavior, thin-walled plates, composite-reinforced metal structures, theory of orthotropic materials, GLARE®**

SPRĘŻYSTO-PLASTYCZNA ANALIZA ZACHOWANIA LAMINATU KOMPOZYTOWO-METALOWEGO PODCZAS OBCIĄŻANIA ORAZ ODCIĄŻANIA

Polimerowe kompozyty włókniste oraz stopy aluminium stanowią obecnie jedne z najczęściej stosowanych materiałów w przemyśle lotniczym. Artykuł przybliża podstawy teoretyczne oraz prezentuje wyniki obliczeń numerycznych dla analizy sprężysto-plastycznej wybranego laminatu kompozytowo-metalowego. Artykuł podaje szczegółowe rozwiązanie analityczna dla wielowarstwowej struktury poddanej cyklowi obciążenia/odciążenia oraz opisuje procesy związane z narastaniem naprężeń i odkształceń. Zauważono, że w płytach GLARE® poddanych jednoosiowemu rozciąganiu istnieje możliwość wystąpienia maksymalnych obciążeń w warstwach metalu podczas odciążania. Można także oczekiwać rozwarstwienia oraz wyboczenia zewnętrznych warstw aluminium. Artykuł, stosując teorię plastyczności, podaje rozwiązanie analityczne konieczne do wyjaśnienia zachowania opisywanej struktury, prezentuje rezultaty obliczeń oraz porównuje je z wynikami analiz numerycznych oraz prac doświadczalnych.

Słowa kluczowe: **model elastoplastyczny materiału, teoria płyt cienkich, struktury kompozytowo-metalowe, własności ortotropowe, GLARE®**

INTRODUCTION

Thin-walled plates and cylinders subjected to mechanical loading are common structural elements used in various industries. For centuries, multi-layered steel tubes for example, have played a major role in a wide range of applications including barrel cannons and pressure or vacuum chambers. With the increasing use of composite materials in various sectors of industry, the need for multi-layered composite structures has become more evident. However, due to the complex mechanical behavior of such as structures, which, for example, exhibit complex modes of deformation, their theoretical analysis requires a slightly different approach. The fundamental theoretical background for analysing anisotropic bodies was provided by Lakhnitskii [1], and his work has been referenced in a large number of textbooks dealing with composites [2-5]. Some specific cases of balanced composites have been studied by Niezgoda and Klasztorny [6], followed by Lewiński and Wilczyński [7], who derived stress-strain relations and material constants for diagonal laminates. Furthermore, hybrid structures like fiber reinforced metal (FRM), or fiber metal laminates (FML) are of interest, [8, 9]. Nowak and Schmidt [10] showed, for example, the mechanism of internal load distribution between thin-walled composite reinforcement and a steel liner working in its elastic-plastic regime.

The potential of composite materials for modern lightweight applications has been known for many years, especially in the aerospace industry. For example, hybrid materials such as composite metal lami-

nates, offer great potential to substitute "pure" metals. GLARE is composed of alternate layers of aluminum and glass fiber-reinforced epoxy (GFRP). Recently, GLARE has been successfully adopted for large parts of the Airbus A380 fuselage, and is also considered as a fan-blade containment material for aircraft turbines. Consequently, detailed understanding and modeling the material response of the composite-metal structure is very important. While the global mechanical response of this material has been extensively experimentally characterized [11, 12], attempts to explain its deformation and buckling modes are limited. In this context, the work done by Bienias et al. [13] has to be mentioned. These researchers analyzed the post-yield behavior of fiber metal laminates composed of aluminum and carbon fibers having a cross-ply stacking sequence, and they noticed that such systems could exhibit delamination and buckling of the external metal layers during unloading.

The work described in this paper tries to explain the mechanical phenomena observed empirically. The paper is formatted as follows: Section Theoretical Background presents the theoretical background and the proposed analytical calculation approach method giving insight into the material models and constitutive relations. Section Analytical Calculation Model covers the numerical example, while the concluding remarks are gathered in the last section of the work.

THEORETICAL BACKGROUND

Classical Lamination Theory

In the conventional approach to lamination [2-5], the stress-strain relation is characterized by an equivalent generalized force (N, M) - generalized strain (ε_0, κ) system:

$$\begin{Bmatrix} N \\ M \end{Bmatrix} = \begin{bmatrix} A & B \\ B & D \end{bmatrix} \begin{Bmatrix} \varepsilon^0 \\ \kappa \end{Bmatrix} \tag{1}$$

where: N, M are vectors of forces and moments, respectively; ε_0, κ are vectors of strains due to the forces and moments, respectively; and A, D and B are called the *tension stiffness*, *bending stiffness* and *coupling stiffness* matrices respectively.

These matrices are calculated as follows:

$$[A, B, D] = \int_{-t_i/2}^{t_i/2} [K_i](1, z, z^2)\,dz \tag{2}$$

where $[K_i]$ is the stiffness matrix of a single i-th lamina, which is spaced from the neutral axis of the laminate by distance z, whereas t_i is the total thickness of the ply.

Normally, the composite may consist of several plies, then the global stiffness matrix $[K_G]$ for the whole structure is calculated with respect to the thickness of individual plies:

$$[K_G] = \frac{1}{t}\sum_i^N t_i [K_i] \tag{3}$$

where: t_i - thickness of i-th ply, t - total thickness of all N plies.

If required, the equivalent mechanical properties of a multi-layer composite may be calculated by simple operations performed on the components of the compliance matrix $[S_G]$, which is the inverse of the global stiffness matrix, $[K_G]^{-1}$:

$$[K_G]^{-1} = [S_G] \rightarrow \begin{cases} \overline{E}_X = \dfrac{1}{s_G^{11}} & \overline{\nu}_{YX} = -\dfrac{s_G^{12}}{s_G^{22}} & \overline{\eta}_{XY} = \dfrac{s_G^{13}}{s_G^{33}} \\ \overline{\nu}_{XY} = -\dfrac{s_G^{21}}{s_G^{11}} & \overline{E}_Y = \dfrac{1}{s_G^{22}} & \overline{\mu}_{XY} = \dfrac{s_G^{23}}{s_G^{33}} \\ \overline{\eta}_X = \dfrac{s_G^{31}}{s_G^{11}} & \overline{\mu}_Y = \dfrac{s_G^{32}}{s_G^{22}} & \overline{G}_{XY} = \dfrac{1}{s_G^{33}} \end{cases} \tag{4}$$

The matrix $[B]$, appearing in Eq. (1), plays an important role in the lamination theory because it causes complex interaction between the in-plane loads and the bending effects. However, composite structures are typically designed in such a way that all the components of $[B]$ are zero, therefore tension-bending coupling does not exist. In this case, coupling factors η and μ in the corresponding directions also are zeroed.

ANALYTICAL CALCULATION MODEL

The classical lamination theory allows transformation of the stiffness of all plies into the global stiffness matrix, and the method works perfectly within the elastic range. However, in the case of elastic-plastic behavior this technique does not offer a simple solution. For this reason, separating the plies working in the elastic range only (composite), and the layers exhibiting elastic-plastic properties (metal) is proposed. In addition, the simple deformation theory of Hencky and Ilyushin will be used to describe the behavior of the metal.

Let us consider a symmetrical and balanced structure, subjected to an in-plane load and having n plies, which can be grouped into metal (1) and composite (2) materials, as shown schematically in Figure 1.

On the basis of the equilibrium relation, it is possible to state:

$$\begin{cases} e_1\sigma_{1X} + e_2\sigma_{2X} = f_X \\ e_1\sigma_{1Y} + e_2\sigma_{2Y} = f_Y \\ e_1\tau_{1XY} + e_2\tau_{2XY} = f_{XY} \end{cases} \tag{5}$$

where f is the distributed force in respective directions [N/mm], e_i - total thickness [mm] of the metal and composite materials, σ, τ are the mean stresses within the materials in respective directions [MPa].

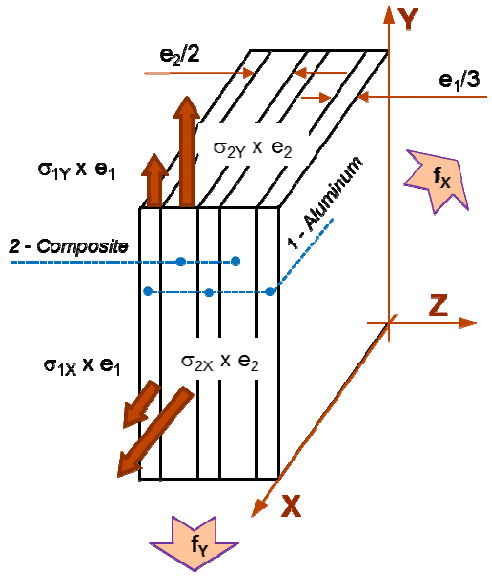

Fig. 1. Geometrical model of the analyzed structure
Rys. 1. Model geometryczny analizowanej struktury

The constitutive equations for an orthotropic material may be found in many textbooks [2-5], and the compliance form of the generalized Hook Law for flat and symmetrical composite layouts can be given as:

$$\begin{Bmatrix} \varepsilon_{iX} \\ \varepsilon_{iY} \\ \gamma_{iXY} \end{Bmatrix} = \begin{vmatrix} 1/E_{iX} & -\nu_{iYX}/E_{iY} & \eta_{iXY}/G_{iXY} \\ -\nu_{iXY}/E_{iX} & 1/E_{iY} & \mu_{iXY}/G_{iXY} \\ \eta_{iX}/E_{iX} & \mu_{iY}/E_{iY} & 1/G_{iXY} \end{vmatrix} \begin{Bmatrix} \sigma_{iX} \\ \sigma_{iY} \\ \tau_{iXY} \end{Bmatrix} + \begin{Bmatrix} \varepsilon^0{}_{iX} \\ \varepsilon^0{}_{iY} \\ \gamma^0{}_{iXY} \end{Bmatrix} \tag{6}$$

where ε and γ are the strains; E, G are the values of the Young and Kirchhoff modules, respectively; ν is Poisson's ratio, while η and μ are the coupling factors in corresponding directions. Initial strains ε^0 may consist of thermal strain components or/and any residual strains.

When considering the whole hybrid structure, one has to assume a perfect bonding between the materials:

$$\begin{cases} \varepsilon_{1X} = \varepsilon_{2X} \\ \varepsilon_{1Y} = \varepsilon_{2Y} \\ \gamma_{1XY} = \gamma_{2XY} \end{cases} \tag{7}$$

Assuming further the cross-ply layout of the composite ($\eta_{XY} = \mu_{XY} = \eta_X = \mu_Y = 0$), and introducing (6) into (7), it is possible to state:

$$\begin{cases} \dfrac{1}{E_{1X}}\sigma_{1X} - \dfrac{\nu_{1YX}}{E_{1Y}}\sigma_{1Y} + \varepsilon^0_{1X} = \dfrac{1}{E_{2X}}\sigma_{2X} - \dfrac{\nu_{2YX}}{E_{2Y}}\sigma_{2Y} + \varepsilon^0_{2X} \\ -\dfrac{\nu_{1XY}}{E_{1Y}}\sigma_{1X} + \dfrac{1}{E_{1Y}}\sigma_{1Y} + \varepsilon^0_{1Y} = -\dfrac{\nu_{2XY}}{E_{2Y}}\sigma_{2X} + \dfrac{1}{E_{2Y}}\sigma_{2Y} + \varepsilon^0_{2Y} \\ \dfrac{\tau_{1XY}}{G_{1XY}} + \gamma^0_{1XY} = \dfrac{\tau_{2XY}}{G_{2XY}} + \gamma^0_{2XY} \end{cases} \tag{8}$$

Relations (5) and (8) constitute a simple system of 6 equations, with the same number of unknowns (σ_{1X}, σ_{1Y}, τ_{1XY}, σ_{2X}, σ_{2Y}, τ_{1XY}):

$$\begin{Bmatrix} \sigma_{1X} \\ \sigma_{1Y} \\ \tau_{1XY} \\ \sigma_{2X} \\ \sigma_{2Y} \\ \tau_{2XY} \end{Bmatrix} = \begin{bmatrix} e_1 & 0 & 0 & e_2 & 0 & 0 \\ 0 & e_1 & 0 & 0 & e_2 & 0 \\ 0 & 0 & e_1 & 0 & 0 & e_2 \\ \dfrac{1}{E_{1X}} & -\dfrac{\nu_{1YX}}{E_{1Y}} & 0 & -\dfrac{1}{E_{2X}} & \dfrac{\nu_{2YX}}{E_{2Y}} & 0 \\ -\dfrac{\nu_{1XY}}{E_{1Y}} & \dfrac{1}{E_{1Y}} & 0 & \dfrac{\nu_{2XY}}{E_{2Y}} & -\dfrac{1}{E_{2Y}} & 0 \\ 0 & 0 & \dfrac{1}{G_{1XY}} & 0 & 0 & -\dfrac{1}{G_{2XY}} \end{bmatrix}^{-1} \begin{Bmatrix} f_X \\ f_Y \\ f_{XY} \\ \varepsilon^0_{2X} - \varepsilon^0_{1X} \\ \varepsilon^0_{2Y} - \varepsilon^0_{1Y} \\ \gamma^0_{2Y} - \gamma^0_{1Y} \end{Bmatrix} \tag{9}$$

Equation (9) describes the general behavior of the cross-ply composite structure subjected to in-plane load and initial strains.

In the case of the analyzed GLARE material, which is exposed to unidirectional tension only (no transverse load or shear, no residual/thermal strains), and introducing equivalent properties for all the fiber reinforced plies, the comprehensive equation (9) can be significantly simplified, and the closed-form solution could be proposed:

$$\begin{bmatrix} \sigma_{1X} \\ \sigma_{1Y} \\ \sigma_{2X} \\ \sigma_{2Y} \end{bmatrix} = \frac{f_X}{k} \begin{bmatrix} e_1 E'\left(1 - \overline{\nu}_{XY}\overline{\nu}_{YX}\right) + e_2 \overline{E}_Y \left(1 - \nu' \overline{\nu}_{YX}\right) \\ e_2 \overline{E}_Y \left(\nu' - \overline{\nu}_{XY}\right) \\ e_1 \overline{E}_X \left(1 - \nu' \overline{\nu}_{YX}\right) + e_2 \dfrac{\overline{E}_X \overline{E}_Y}{E'} \left(1 - \nu'^2\right) \\ -e_1 \overline{E}_X \left(\nu' - \overline{\nu}_{YX}\right) \end{bmatrix} \tag{10}$$

and:

$$k = e_1^2 E'\left(1 - \overline{\nu}_{XY}\overline{\nu}_{YX}\right) + e_2^2 \frac{\overline{E}_X \overline{E}_Y}{E'}\left(1 - \nu'^2\right) + e_1 e_2 \left[\overline{E}_X \left(1 - \nu' \overline{\nu}_{YX}\right) + \overline{E}_Y \left(1 - \nu' \overline{\nu}_{XY}\right)\right]$$

where index "1" and the "prime" sign refer to the metal, and index "2" and the "dash" sign refer to the composite equivalent proprieties, respectively.

Knowing the equivalent stress within the composite, σ_2, the stresses in the particular layers σ_i can be found by:

$$\begin{Bmatrix} \sigma_{iX} \\ \sigma_{iY} \\ \gamma_{iXY} \end{Bmatrix} = \left[K_i\right]\left[K_G\right]^{-1} \begin{Bmatrix} \sigma_{2X} \\ \sigma_{2Y} \\ \gamma_{2XY} \end{Bmatrix} \tag{11}$$

EQUIVALENT MATERIAL PROPERTIES

In order to describe the material properties of aluminum, which change during the progress of plastic deformation, one can take advantage of the simple deformation theory provided by Hencky and Ilyushin. They postulated that for "nearly" proportional loads, the total strain (the sum of elastic and plastic components) is given as a function of total stress (Fig. 2).

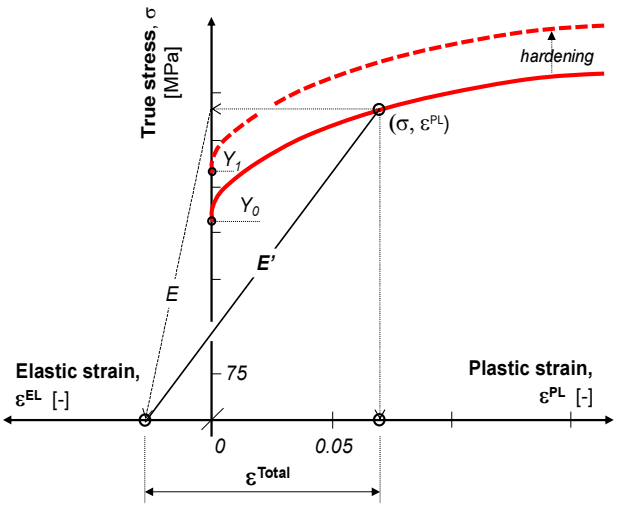

Fig. 2. Elastic-plastic behavior of T3 aluminum

Rys. 2. Wykres rozciągania aluminium T3 w zakresie elastoplastycznym

In this case the calculation model, as described by equation (10), can also be used in the elastic-plastic regime, if the elastic properties of the metal are replaced by their equivalent forms:

$$E' = \frac{\sigma_{Mises}}{\varepsilon_{EL} + \varepsilon_{PL}} = \frac{E\sigma_{Mises}}{\sigma_{Mises} + E\varepsilon_{PL}}$$
$$\upsilon' = \frac{1}{2}\left[1 - \frac{E'}{E}(1 - 2\upsilon)\right] \tag{12}$$

where E' is the secant value of Young's modulus, and ν' is the corresponding Poisson's ratio. E, ν - aluminum properties within the elastic limit (E = 70GPa, ν = 0.32)

In the absence of a shear load, the equivalent (von Mises) stress and equivalent plastic strains are defined as follow:

$$\sigma_{Mises} = \sqrt{\sigma_{1X}^2 - \sigma_{1X}\sigma_{1Y} + \sigma_{1Y}^2} \tag{13}$$

$$\varepsilon_{PL} = \frac{2}{\sqrt{3}}\sqrt{\varepsilon_X^{PL\,2} + \varepsilon_Y^{PL\,2} + \varepsilon_Z^{PL\,2}} \tag{14}$$

According to the deformation theory of Hencky and Ilyushin, the total strains of the material working in the elastic-plastic regime can be described as:

$$\begin{bmatrix} \varepsilon_X^{Total} \\ \varepsilon_Y^{Total} \\ \varepsilon_Z^{Total} \end{bmatrix} = \frac{1}{E'}\begin{bmatrix} \sigma_{1X} - \upsilon'\sigma_{1Y} \\ \sigma_{1Y} - \upsilon'\sigma_{1X} \\ -\upsilon'(\sigma_{1X} + \sigma_{1Y}) \end{bmatrix} \tag{15}$$

If the elastic-plastic properties (E' and ν') are replaced by metal properties within the elastic limit (E, ν), the elastic strain components may be calculated in a very similar manner:

$$\begin{bmatrix} \varepsilon_X^{EL} \\ \varepsilon_Y^{EL} \\ \varepsilon_Z^{EL} \end{bmatrix} = \frac{1}{E}\begin{bmatrix} \sigma_{1X} - \upsilon\sigma_{1Y} \\ \sigma_{1Y} - \upsilon\sigma_{1X} \\ -\upsilon(\sigma_{1X} + \sigma_{1Y}) \end{bmatrix} \tag{16}$$

Naturally, the total strain is the sum of elastic and plastic strains, in respective directions. Therefore:

$$\begin{bmatrix} \varepsilon_X^{PL} \\ \varepsilon_Y^{PL} \\ \varepsilon_Z^{PL} \end{bmatrix} = \begin{bmatrix} \varepsilon_X^{Total} \\ \varepsilon_Y^{Total} \\ \varepsilon_Z^{Total} \end{bmatrix} - \begin{bmatrix} \varepsilon_X^{EL} \\ \varepsilon_Y^{EL} \\ \varepsilon_Z^{EL} \end{bmatrix} \tag{17}$$

Calculating the equivalent properties of the composite structure is more straightforward, and follows the procedure described by equations (3) and (4).

CALCULATION PROCEDURE

Analysis within the elastic limit can be managed with the help of equation (10), if the elastic properties of the metal are simply used ($E' = E$, $\nu' = \nu$). The plastic regime requires, however, the strain control. In this case a test point (σ_{Mises}, ε^{PL}) on the stress - plastic strain curve (Fig. 2), needs to be selected, and corresponding equivalent properties of the metal should be calculated according to Eq. (12). Next, the distributed tensile force, f_X, matching the specified test point, may be derived from:

$$f_X^{(test)} = \sigma_{Mises}\frac{k}{\sqrt{k_X^2 - k_X k_Y + k_Y^2}} \tag{18}$$

where:

$$k_X = e_1 E'(1 - \overline{\nu}_{XY}\overline{\nu}_{YX}) + e_2\overline{E}_Y(1 - \nu'\overline{\nu}_{YX})$$
$$k_Y = e_2\overline{E}_Y(\nu' - \overline{\nu}_{XY})$$
$$k = e_1^2 E'(1 - \overline{\nu}_{XY}\overline{\nu}_{YX}) + e_2^2\frac{\overline{E}_X\overline{E}_Y}{E}(1 - \nu'^2) + \tag{19}$$
$$+ e_1 e_2\left[\overline{E}_X(1 - \nu'\overline{\nu}_{YX}) + \overline{E}_Y(1 - \nu'\overline{\nu}_{XY})\right]$$

Knowing the tensile force, the stress components for the metal and composite layers can be calculated from Eq. (10), and for the specific plies - from Eq. (11). It must also be noted that the tensile force required to reach the elastic limit of the multi-layered structure may be found, if one introduces $\sigma_{Mises} = Y_0$ (which is about 337 MPa for T3 aluminum) into Eq. (18).

When releasing the tensile load, the structure will try to return to the initial shape. However, the aluminum layers are hardened already during loading. Therefore, in order to properly describe the unloading step, the original strain-stress curve needs to be corrected. Assuming the isotropic hardening principle, the yield surface will keep the same shape, but should expand with increasing stress. Practically it means, that the "true stress-plastic strain" curve, as shown in Figure 2, has to be shifted vertically, from the original yield point Y_0, to the maximum von Mises stress reached at loading, Y_1.

In practice, the unloading procedure may be treated as a separate step - compression of the stress-free sam-

ple having the original geometry, but hardened material. The final state could be characterized by the algebraic sum of the results (total stresses and strains) produced in two steps: (I) tensile of the virgin material, and (II) compression of the already hardened material. However, it is important to note that the von Mises yield surface, which is needed to describe the stress-strain behavior (Fig. 2), takes now the form:

$$f(\sigma_{Mises}) = \sqrt{\sigma'^2_{1X} - \sigma'_{1X}\,\sigma'_{1Y} + \sigma'^2_{1Y}} \tag{20}$$

and:

$$\sigma'_i = \sigma_i + \alpha_i \tag{21}$$

where σ'_i is the actual stress in respective directions; σ_i - is the compressive stress calculated in the "unloading" step, and α_i is the tensile stress at the end of the loading step (often called the *backstress*).

More details on the calculation procedure can be found in [14, 15].

NUMERICAL EXAMPLE

The analyzed geometry of the GLARE plate consisted 3 layers of aluminum, which were separated by cross-ply (0/90) layers of carbon fiber (CF) composite (Fig. 3). The material properties of a single fiber-reinforced layer could be estimated as: E_T=134 GPa, E_L = 9.7 GPa, ν_{TL} = 0.29, ν_{LT} = 0.02, and G_{TL} = 3.5 GPa. It corresponds to the equivalent properties for the whole cross-ply composite structure as: E_X = E_Y = 77.2 GPa, ν_{XY} = ν_{YX} = 0.04, and G_{XY} = 3.5 GPa.

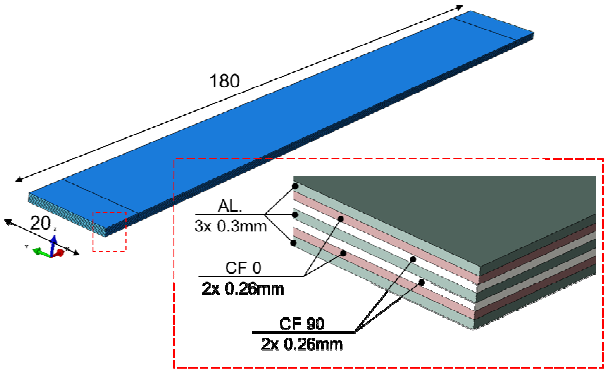

Fig. 3. Geometrical model of analyzed FML sample

Rys. 3. Model geometryczny analizowanej próbki FML

The test sample was subjected to tension in the X direction, with force F_X = 33.5KN, and next unloaded.

The numerical calculations were performed using the provided analytical model, as described in Section Theoretical Background, as well as by the finite element method, with the help of the ABAQUS simulation package [16]. Both approaches gave very consistent results. For example, at the end of the loading phase, the analytical approach predicted stresses in the load direction: σ_X = 2318 MPa for CF 0, and σ_X = = 162.7 MPa for CF 90, while the FEM software returned 2317 and 162.3 MPa, respectively. More interesting is the situation in the Y direction because due to orientation of the CF 90 plies, these layers exhibit compression (–274 MPa), while the CF0 plies show negligible tension (26 MPa) - at the end of the loading phase. The situation is much more complex for aluminum, especially during the unloading phase. As shown in Figure 4, at the end of the loading phase the stress in the X direction reaches 431 MPa, which corresponds to 380 MPa of the equivalent von Mises stress. At this stage, the total strain in the X direction of 1.72% is comprised of the elastic component (0.52%), and substantial plastic strain (1.20%).

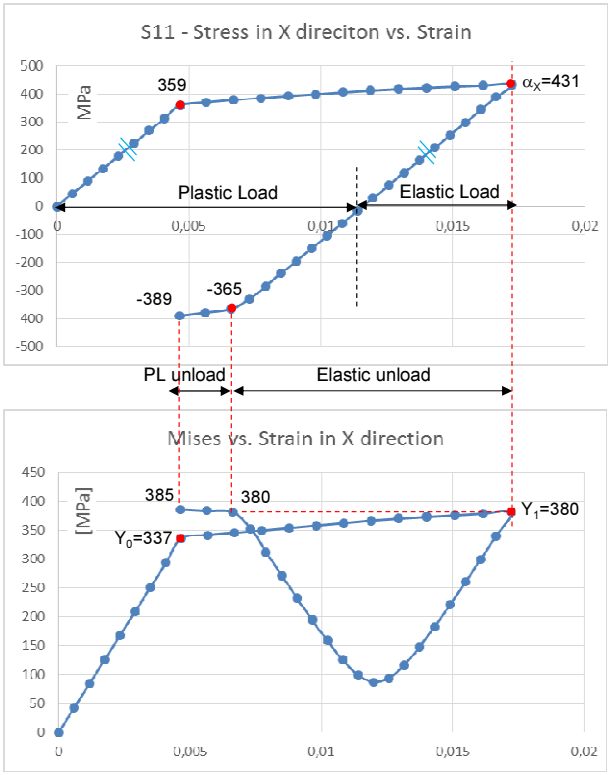

Fig. 4. Stresses vs. strains in X direction for aluminum during loading and unloading phases. Top picture presents stress in X direction, while bottom shows von Mises stress

Rys. 4. Naprężenia jako funkcja odkształceń w osi wzdłużnej dla aluminium podczas obciążania i odciążania. Górna krzywa opisuje naprężenia w kierunku X, a dolna naprężenia ekwiwalentne Misesa

During unloading, the stress in the X direction and von Mises stress are reduced first. Nevertheless, due to the hardening achieved as a result of plastic flow during loading, the stress in the X direction can elastically progress even to negative values, unless the von Mises stress reaches the same plastic state of 380 MPa. Starting from this point, further unloading is managed using plastic deformations until force balance conditions for the aluminum and composite layers are met. Thus, in the second phase, the elastic strain was reduced by 1.05% (reaching –0.53%), while the plastic strain was reduced by –0.20% (reaching 1.00%). At the end of the

process the von Mises stress (385 MPa) is a bit higher than at the start of loading, aluminum is exposed to significant compression (–389 MPa), and there are still some total residual strains in the X direction at the level of 0.47%. Naturally, since all the layers are tied, the same strain applies to composite plies, leading to compression of the aluminum and tension in the composite. While aluminum is exposed to a negative stress of –389 MPa at the end of the unloading process, the corresponding reaction force is mainly managed by two plies of CF 0, which, due to a much lower total thickness, are subjected to a positive stress of 628 MPa. The remaining plastic strain in aluminum (1.00%), complex mismatching in stresses (compression in aluminum and tension in the composite), as well as unbalanced force conditions for the external layers, are the main reasons for the phenomena observed experimentally by Bienias et al.

The main results are presented in Table 1.

TABLE 1. **Summary of results**
TABELA 1. **Podsumowania wyników**

		Analytical				*FEM*
		ε_X^{EL} [%]	ε_X^{PL} [%]	σ_X [MPa]	σ_{Mises} [MPa]	σ_{Mises} [MPa]
LOAD	Alum	*0.52*	*1.20*	431	380.4	380.2
	CF_0	*1.72*		2318	2305	2305
	CF90			163	382	407
UNLOAD	Alum	*–1.05*	*-0.20*	–820	756	
	CF_0	*–1.26*		–1690	1683	
	CF90			–117	351	
END	Alum	*–0.53*	*1.00*	–389	384.6	385.3
	CF_0	*0.47*		628	622	619
	CF90			44	44	46

The calculated results also match the measured ones. The stress in the X direction at the end of loading (431 MPa for AL, 2138 MPa for CF0 and 163 MPa for CF90), averaged over the thickness reached the level of 865.0 MPa, which corresponds very well to the measured data of 865.72 MPa, as reported by Bienias. A small difference is seen in the strain results: 1.72% as calculated vs. 1.84% as measured. This minor deviation (6.5%) can be, however, attributed to the differences in material properties (assumed, and real ones), and the small amount of thermal strains which could exist after the manufacturing process.

CONCLUSIONS

The paper presented the structured approach for the analysis of fiber metal laminates working in the elastic-plastic regime. The analytical model combining the classical lamination theory with the deformation theory by Hencky-Ilyushin was introduced first, then the closed-form solution was proposed. The numerical calculation case which was managed provided deeper insight into the mechanical phenomena of FML structures, and allowed the author to explain the complex interaction between the aluminum and composite layers. It was concluded that if plastic strains appear during loading, one may expect significant stresses at the end of unloading in FML structures. Thus, both the design and exploitation of GLARE plates should be managed keeping in mind the mechanical phenomena studied in this article.

REFERENCES

[1] Lekhnitskii S.G., Theory of Elasticity of an Anisotropic Body (English translation), Mir Publishers, Moscow, 1981.
[2] Gay D., Hoa S.V., Tsai S.W., Composite Materials: Design and Applications, CRC Press, 2002.
[3] Jones R., Mechanics of Composite Materials 2nd ed., CRC Press, 1998.
[4] Herakovitch C., Mechanics of Fibrous Composites, John Wiley & Sons, New York 1998.
[5] Crawford R.J., Plastics Engineering, Elsevier 2002.
[6] Niezgoda, T., Klasztorny, M., Homogenization theory of regular cross-ply laminates, Composites 2009, 9:2, 154--158.
[7] Lewiński J., Wilczyński A., Symmetric, balanced cross-ply and diagonal-ply laminates, Global elastic properties and internal stresses, Composites 2010, 10, 1, 1-45.
[8] Lifshitz J.M., Dayan H.M., Filament-wound pressure vessel with thick metal line, Comp. Struct. 1995, 32, 313-323.
[9] Xia M., Kemmochi K., Takayanagi H., Analysis of filament-wound fiber-reinforced sandwitch pipe under combined internal pressure and thermomechanical loading, Comp. Struct. 2001, 51, 273-283.
[10] Nowak T., Schmidt J., Prediction of elasto-plastic behavior of pressurized composite reinforced metal tube by means of acoustic emission measurements and theoretical investigation, Composite Structures 2014, 118, 49-56.
[11] Wu G.C., Yang J.M., The mechanical behavior of GLARE laminates for aircraft structures, JOM 2005, 57, 1, 72-79.
[12] Gerlach R., Siviour C.R., Wiegand J., Petrinic N., The strain rate dependent material behavior of S-GFRP extracted from GLARE, Mechanics of Advanced Materials and Structures 2013, 20, 505-514.
[13] Bienaś J., Majerski, K., Surowska, B., Jakubczak, P., The mechanical properties and failure analysis of selected fiber metal laminates, Composites Theory and Practice 2013, 13, 3, 220-224.
[14] Nowak T., Homogenization of fiber metal laminate structures characterized by orthotropic and elastic-plastic material models, Computer Methods in Materials Science 2015, 1, 169-175.
[15] Nowak T., Elastic-plastic behavior and failure analysis of selected fiber metal laminates, Composite Structures (in press), https://doi.org/10.1016/j.compstruct.2017.05.007
[16] ABAQUS/Standard User's Manual; Habit, Karlson & Sorenson, Inc., Pawtucket, RI, 2010.

